Please, cite as: De Matteis, G., Sarracco, G., & Brando, G. (2016). Experimental tests and optimization rules for steel perforated shear panels. Journal of Constructional Steel Research, 123, 41-52. doi:10.1016/j.jcsr.2016.04.025

EXPERIMENTAL TESTS AND OPTIMIZATION RULES FOR STEEL PERFORATED SHEAR PANELS

Gianfranco De Matteis[1], **Gianluca Sarracco and Giuseppe Brando**

Department of Engineering and Geology (INGEO), University "G d'Annunzio" of Chieti-Pescara, Italy

ABSTRACT

This paper presents the main results obtained downstream an experimental and numerical study carried out on steel perforated shear panels.

In a first stage the experimental response of the studied is analysed, aiming at assessing the dissipative capacity. The main observed experimental evidences allow to point out that the hysteretic cycles could be detrimentally influenced by pinching effects and cumulated damage. Such phenomena are mainly due to unexpected lateral-torsion buckling that arises when the plate portions delimited by perforations are too much slender. Then, a suitable analytical formulation for the prediction of the strength at several shear demands, accounting for the influence of the above negative effects, is provided.

The second part of the manuscript presents a parametric study based on a FEM numerical model calibrated on the basis of the experimental tests. Two goals are achieved: *i*) to establish the influence of the main geometric parameters on the panel hysteretic response, with particular regard to the pinching effects provoked by buckling phenomena; *ii*) to provide analytical formulations able to give back the ratio between the "pinching" strength and the maximum strength, the former being the force corresponding to a null shear strain in a cycle. These formulations are proposed as a suitable predictive tool for determining the optimal perforation geometry to be assigned to the panel depending on the expected shear demand.

Keywords: Steel Shear Walls, Perforated Shear Plates, Dampers, Seismic Protection, Pinching, Experimental Tests, Design rules, Numerical Analysis.

[1]**Corresponding author:** Prof.. Gianfranco De Matteis, Ph.D
Address: Department of Engineering and Geology, University of Chieti-Pescara,
V.le Pindaro 62, 65127- Pescara – ITALY.
Phone: (0039) 085 4537261, Fax: (0039) 0854537255, e-mail: dematteі@unina.it

1. INTRODUCTION

Nowadays, the application of weak metallic shear panels to the frames of new and existing buildings is believed to be a viable and effective way for protecting the main structural members from damage, even under severe seismic shacking. In fact, these systems are able to guarantee, if well conceived, a large dissipative capacity, activated for limited structural demands, due to the high ductility that characterizes both the base material and the resisting mechanism.

The essential prerogative that must be assured for these types of dampers is that their response must not be influenced by the detrimental effects generated by buckling phenomena. These can arise when the base plate is characterized by high local or global slenderness and produce pinched hysteretic cycles.

Several solutions of weak metallic panels have been proposed in the last two decades, also for the retrofitting of existing rc buildings[1-2]. Most of these have been realized by using low yield stress point materials [3]. Nakashima proposed to use a steel type whose 0.2 percent offset yield stress is 120 MPa [4]. De Matteis et al. [5-6] used an almost pure aluminium that, following a heat treatment process, is characterized by a conventional yield stress of 25 MPa and a ductility of about 40% [7]. Similarly, miscellaneous aluminium alloys were profitably used by Rai et al. [8-9]. All the aforementioned studies concerned relatively thin plates on which transversal stiffeners were applied in order to shift the activation of potential buckling phenomena in the inelastic field.

As a convenient alternative, the authors of this paper [10-11] and, later, also Deng et al. [12] proposed to use very thin plates, made of either innovative or traditional materials, for which buckling phenomena are inhibited by special elements that restrain the out-of-plane displacements, but that do not interact with the base plate when it undertakes membrane strains. Such a system applies the basic concept of buckling restrained braces (BRBs) in the bi-dimensional space, offering the same advantages from the dissipative point of view [13], but allowing a more convenient control at collapse because of the post-critical resources of the plate in shear.

More recently, it has been recognized that another fruitful way for obtaining dissipative shear panels consists in weakening the base plate by removing some parts. On the one hand, this solution reduces the shear strength, allowing accomplish more easily the capacity design criteria; on the other, it allows to mitigate the negative effects generated by buckling phenomena by the opportune variation of the internal stress pattern.

In this framing of research, this paper presents the results of an experimental and numerical study carried out on steel perforated shear plates. In particular, the outcomes of two full scale tests are shown, highlighting the most influencing experimental evidences, with particular regard to those phenomena that could reduce the dissipative capacity of the studied devices. Then, the obtained experimental results are used in order to set-up a sophisticated FEM model that is subjected to an extensive parametric analysis that allows to provide design rules to be used for the optimization of the holes configuration.

In synthesis, the research study presented here aims to achieve the following goals:

- To investigate the hysteretic behaviour of very thin perforated shear panels by experimental tests;
- To put in evidence potential detrimental mechanisms under cycles of different amplitude;
- To optimize the panel response, by means of numerical analyses carried out on calibrated FEM models, in terms of perforation geometrical features, also accounting for the thickness of the base plate;
- To propose design formulations that give back the panel configuration according to the expected performance.

2. STATE-OF THE ART

2.1 Experimental studies

The results of experimental tests are very useful to analyse the response of weakened shear panels. In fact the variation of the internal stresses pattern due to the removed portions of plate could lead to unexpected behaviours.

Some interesting experimental analyses on weakened shear panels are present in literature. Hitaka and Matsui [14] tested forty-two shear plates with several vertical slits. The shear force acting on the system is commuted in a bending mechanism for the plate portions confined by two slits, which undergo large flexural deformations producing a significant dissipative capacity. Recently, this type of system has been considered by Pohlenz [15], who studied the influence of slits layout and gave analytical formulations in order to assess the initial stiffness, the maximum strength, the force levels triggering buckling and the dissipated energy.

Vian, Bruneau and Purba [16] carried out experimental tests on shear panels weakened by holes arranged in a staggered configuration. They provided design formulations of the shear strength accounting for the holes diameters and spacing, also considering the influence of the surrounding frame stiffness.

Valizadeh et al. [17] investigated the cyclic response of six 1:6 scaled specimens of perforated shear walls made of plates with a central circular opening. They quantified the influence of the hole diameter on the loss of dissipated energy due to the pinching effects on the hysteretic cycles. Furthermore, they highlighted the presence of brittle failures around the perforations when very thin plates are adopted.

Alavi and Nateghi [18], by experimental tests on 1:2 scaled single-story SPSWs, proved that perforated diagonally stiffened shear panels could allow the same stiffness of un-ribbed solid panels, with an increase of ductility of more than 14%. In addition, an extension of the design formulation of the shear strength given previously by other Authors was provided, accounting for the diagonal stiffeners contribution.

Chan et al. [19] introduced a Perforated Yielding Shear Panel Device (PYSPD), considering three possible layouts of perforation and proving that, for certain plate slenderness, the obtained hysteretic cycles are stable and a high ductility is achievable, with a potential large dissipation capacity that can be exploited under seismic force, in particular for rectangular patterns of perforations.

2.2 Numerical analyses on weakened shear panels

The study of metal perforated shear plates cannot disregard from the use of calibrated FEM numerical models. On the one hand, they allow to well identify the internal stress patterns that arise owing to the perforation layout. On the other hand, they allow the possibility of easily varying the geometrical and mechanical properties to carry out extensive parametric analyses for selecting optimal holes configuration.

Several Researchers investigated the performance of perforated shear panels through FEM models. Purba and Bruneau [20] analysed an entire steel perforated shear wall in which the base plate worked according to a weakened strip model originated from perforations arranged in a staggered configurations. In a first step the Authors performed finite element analyses on local models of single strips weakened by holes with diameters ranging from 10 mm to 300 mm. Then, they considered the model of the whole perforated shear wall in order to investigate the relationship between the perforation diameter and the infill panel strain, in order to verify the accuracy of the individual strip model results and to analyse the influence of the perimeter frame stiffness on the stress/strain of the plate.

Bhowmick [21] performed non linear pushover analyses on series of single storey perforated steel plate shear walls with different aspect ratios and perforation diameters, so to confirm the reliability of an analytical equation able to predict the design shear strength. Moreover, the forces in the surrounding frame members of multi-storey buildings, deriving from the above shear strength, were analysed.

Pellegrino et al. [22] studied the influence of one perforation on both buckling strength and post-critical behaviour of steel plate in shear, accounting for several holes dimensions, shape and positions, as well as considering different plate slenderness and aspect ratios.

In [23], on the basis of the experimental tests carried out by Egorova et al. [24], a numerical model on a steel plate with a pattern of holes leaving ring-shaped portions of steel connected by diagonal links was developed. The dissipative capacity of the system was guaranteed by the plastic mechanism activated when steel circular rings deformed into ellipses; moreover the presence of the diagonal links allowed the mitigation of possible out-of-plane buckling.

3. THE EXPERIMENTAL CAMPAIGN

3.1 Tested shear panels

The two tested Perforated Shear Panels, that henceforth will be referred as PSP1 and PSP2, were made of 2.5 mm thick plates. The geometric features are described in Fig. 1, where the sizes are expressed in mm. Each specimen was obtained by applying nine perforations according to a rectangular pattern. As reported in [19], this type of choice allows better performances with respect to a staggered configuration. Hole diameters of 127.5 mm and 107.4 mm were imposed for PSP1 and PSP2, respectively.

Each plate was connected to a perimeter articulated frame made of four built up members obtained by coupling two UPN 120 channel section profiles. The plate-to-perimeter frame connections were realized by 8.8 grade M14 steel friction bolts spaced by a pitch of 50 mm.

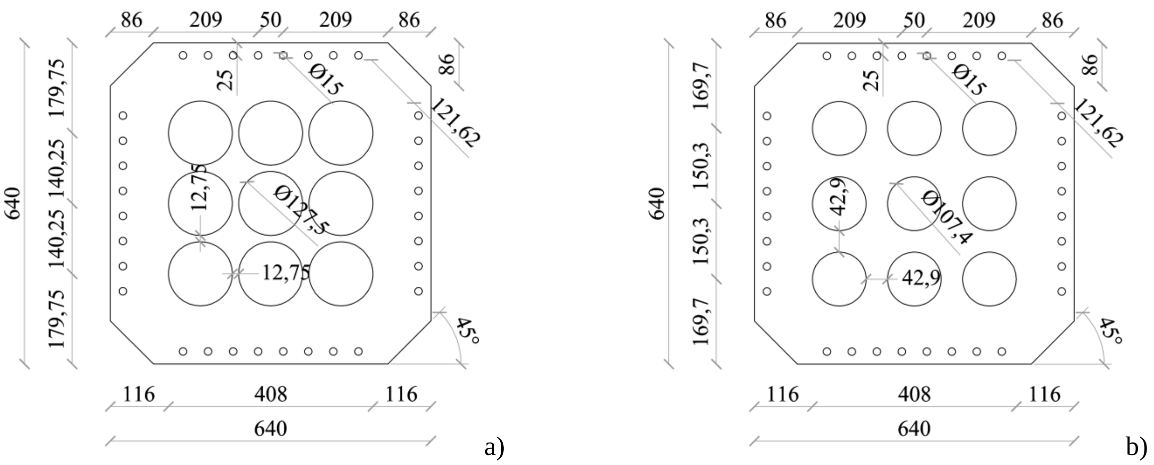

Figure 1. Plate geometry for tested shear panels: (a) PSP1 and (b) PSP2 (sizes in mm).

In addition, in order to increase the contact area between the plate and the built up members, double sided internal 10 mm thick plates (two for each edge of the articulated frame) were applied, as it can be seen in figure 2.a where the panel is shown during the assemblage process.

The experimental set-up was completed by two hinged steel jigs connecting two opposite vertices of the panel to the MTS machine used for carrying out pseudo-static cyclic tests (see Fig. 2b).

The material mechanical properties of the plates were preliminarily investigated by means of uniaxial tensile tests. These were carried out on dog-bone specimens extracted from the same metal sheeting. In particular, four coupons along the lamination direction (named H1, H2, H3 and H4) and other five (V1, V2, V3, V4 and V5) along the perpendicular one were taken out.

a) b)

Figure 2. The experimental set-up: specimen (a) during the assemblage and (b) during the test

The obtained results, reported in Fig. 3 together with the curves fitting the average values and the true strain-true stress, showed that the yield stress measured in the lamination direction (about 300 MPa) differs from the one considered perpendicularly (about 270 MPa), whereas no significant differences were revealed in terms of tangential stiffness and ductility. An anisotropic behaviour at yielding was therefore expected.

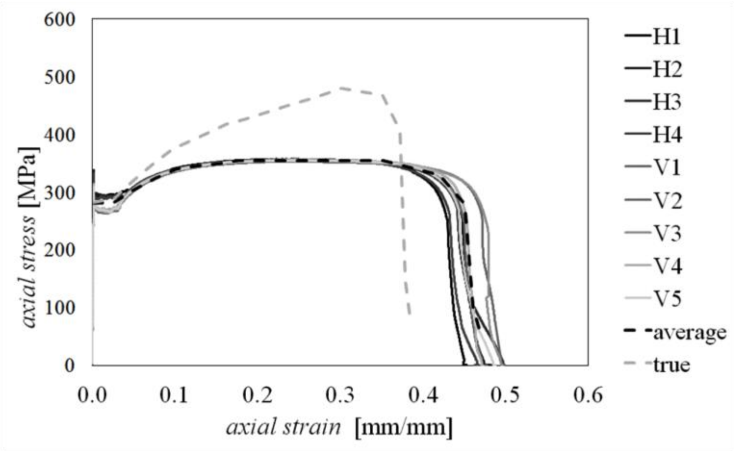

Figure 3. The mechanical stress-strain curves of the tested plate base material (engineeristic and true values)

The two tested perforated shear panels were subjected to pseudo-static cyclic tests, considering a diagonal displacements history consistent with the ECCS Provisions [25] (Fig. 4a).

As already shown in figure 2b, the diagonal displacements of the tested panels were measured by a mechanical transducer, whereas the corresponding diagonal force was appraised by the loading cell installed in the testing machine.

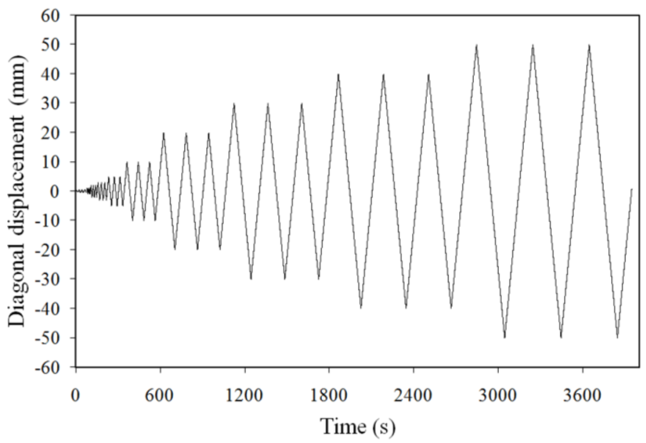

a)

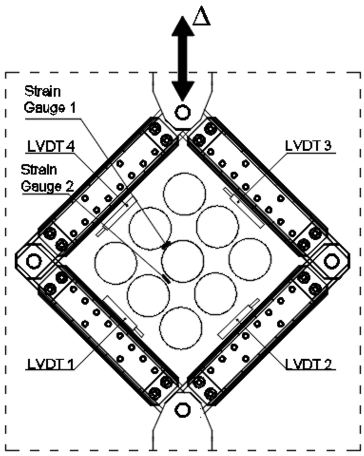

b)

Figure 4. a) The imposed diagonal displacement history; b) the measurement equipment used during tests

Also, four mechanical LVDT transducers were placed on the perimeter of the panels (Fig. 4b), to measure the potential relative motion between the plate edges and the frame elements. Their responses, retrieved during the tests, are described in figure 5.a and 5.b for panel PSP1 and PSP2 respectively. Indeed, some slipping phenomena were registered, but they never exceeded 1.5 mm, resulting not significantly influencing for the shear panel response.

The testing apparatus was completed by two uniaxial strain gauges glued on the central plate portions detected by the perforations, so to monitor the developed material strain.

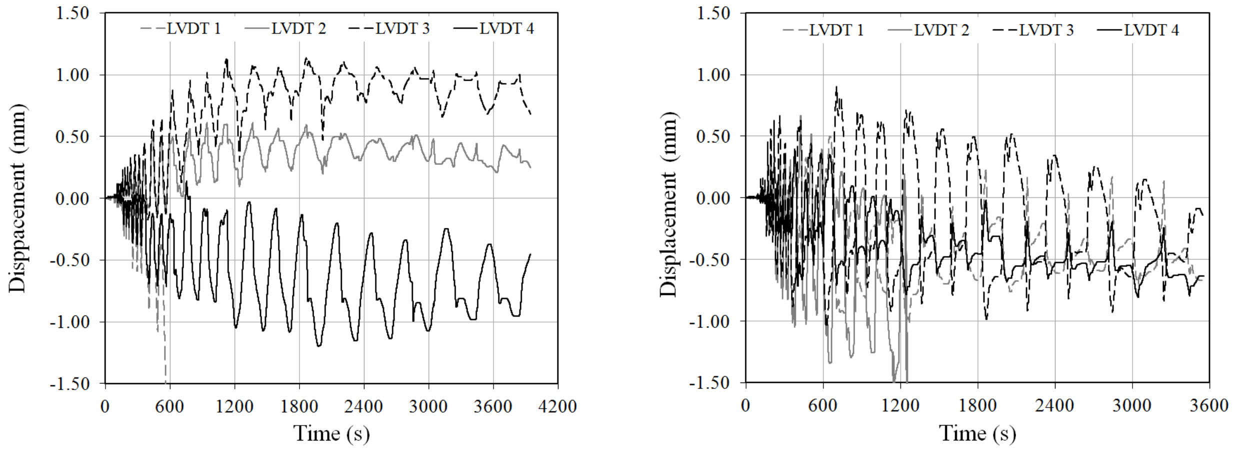

a) b)

Figure 5. The lateral LVDT transducers responses for panel PSP1(a)and PSP2 (b)

3.2 Experimental evidence

Following an initial phase in which the panels behaved as a system under pure shear, the former “global” buckling waves arose in the plate cores centred around the two diagonals. They were triggered at diagonal displacements of ±5mm (shear strain of ±1.1%; figure 6.a) and ±2mm (shear strain of ±0.4%; figure 6,b) for PSP1 and PSP 2, respectively. For the latter, instability phenomena were anticipated due to the lower influence of the perforations. In fact, in this phase, the specimen PSP2 tended to behave more similarly to a not-perforated shear panel than the specimen PSP1, thus resulting more influenced by buckling phenomena.


a)


b)

Figure 6. The first buckling phenomena revealed for (a) the specimen PSP1 at a displacement of ±5.00 mm (shear strain of ±1.1%) and (b) specimen PSP2 at a displacement of ±2.00 mm (shear strain of ±0.4%)

Indeed, as it is shown in the figure, the amplitude of the diagonal buckling waves described above remained fundamentally unchanged for higher shear demands, for both PSP1 and PSP2 specimens, this proving the effectiveness of the perforation pattern in diverting the internal stresses and, therefore, in mitigating those instability effects that commonly develop for solid shear plates.

Nevertheless, when larger diagonal displacements were attained, the activation of higher critical modes was noticed. These modes consisted in lateral-torsional buckling of the panel portions included within the perforations and were due to a rotation of the principal stresses (see Section 4.4). These phenomena were clearly visible for a diagonal displacement of 10mm (shear strain of 2.2%) for both PSP1 and PSP2 specimens, as it is shown in figure 7. The main effects consisted in a twisting of the buckled plates portions, with damage significantly cumulated when the number of cycles increased.

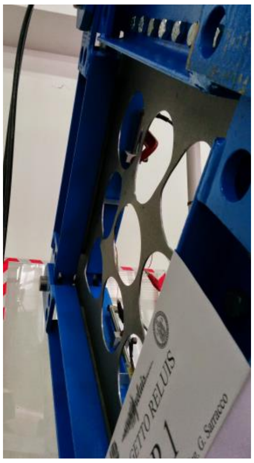
a)

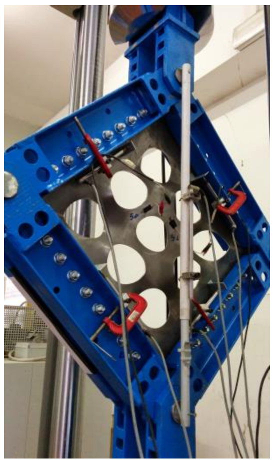
b)

Figure 7. Lateral-torsion buckling of the panel portions included within the perforations activated for a displacement of ±10.00 mm (shear strain of ±2.2%): (a) specimen PSP1 and (b) spacimen PSP2.

When a diagonal displacement of 20 mm (shear strain of 4.4%) was attained the torsion became permanently visible, as shown in Fig. 8.

For higher shear strains, failures due to low cycle fatigue were triggered around the perforations. They influenced the panel performance when diagonal displacements of 30 mm (shear strain of 6.7%) and 40 mm (shear strain of 9.6%) were attained. In figure 9 the plate configurations at this deformation stage are shown.

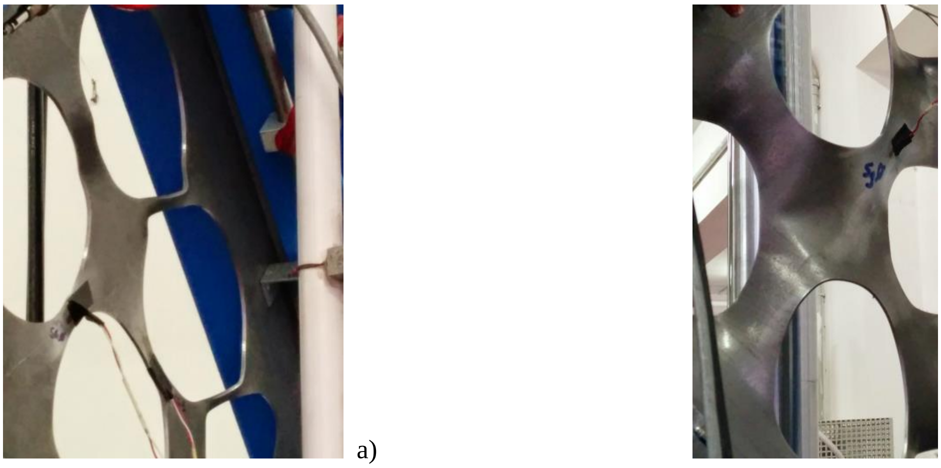
a) b)

Figure 8. The experimental evidences registered for the specimens (a) PSP1 and (b) PSP2 at a diagonal displacement of 20 mm (shear strain of ±4.4%).

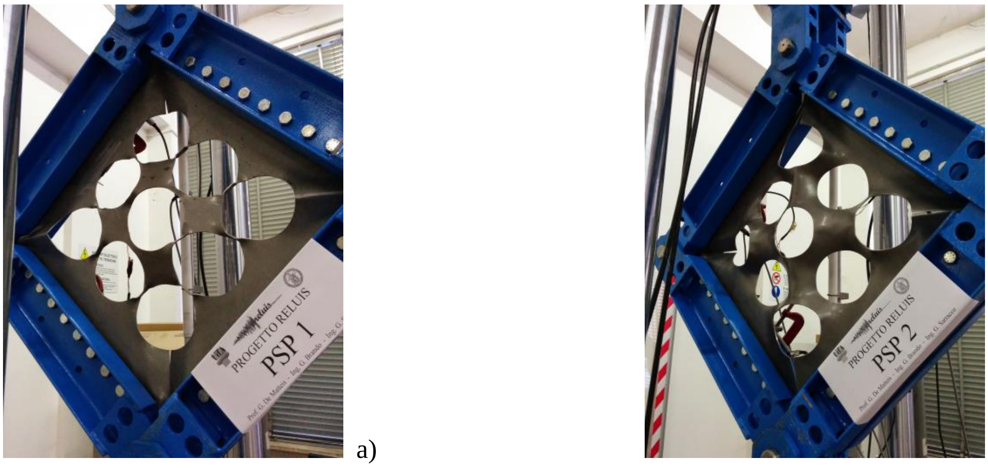

a) b)

Figure 9. The collapse modes of the (a) PSP1 and (b) PSP2 specimens.

3.3 Hysteretic response

The obtained cyclic responses of the two tested shear panels are plotted in Fig. 10 in terms of diagonal displacements vs. diagonal forces. As it can be observed, conspicuous pinching effects were revealed in both cases. These were due to several detrimental phenomena caused by cumulated plastic deformations induced by the local buckling discussed previously which led to a cyclic decay of the maximum strength for each shear demand.

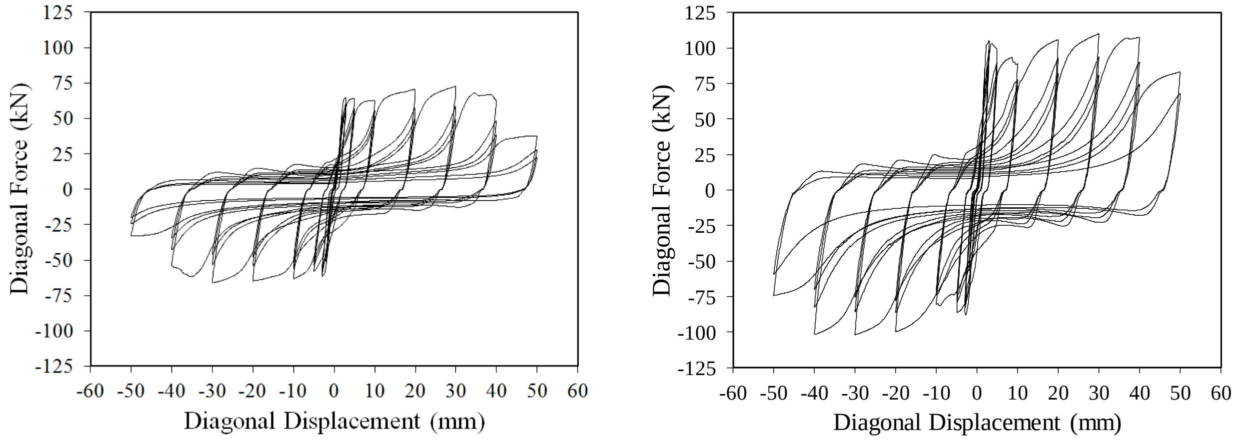

a) b)

Figure 10. The obtained hysteretic cycles for specimen (a) PSP1 and (b) PSP2.

This decay is highlighted in figure 11, where the maximum diagonal forces are plotted. Moreover, in the same figure, the percentage differences between the maximum and the minimum strength (normalised to the maximum one) at each cycle is given.

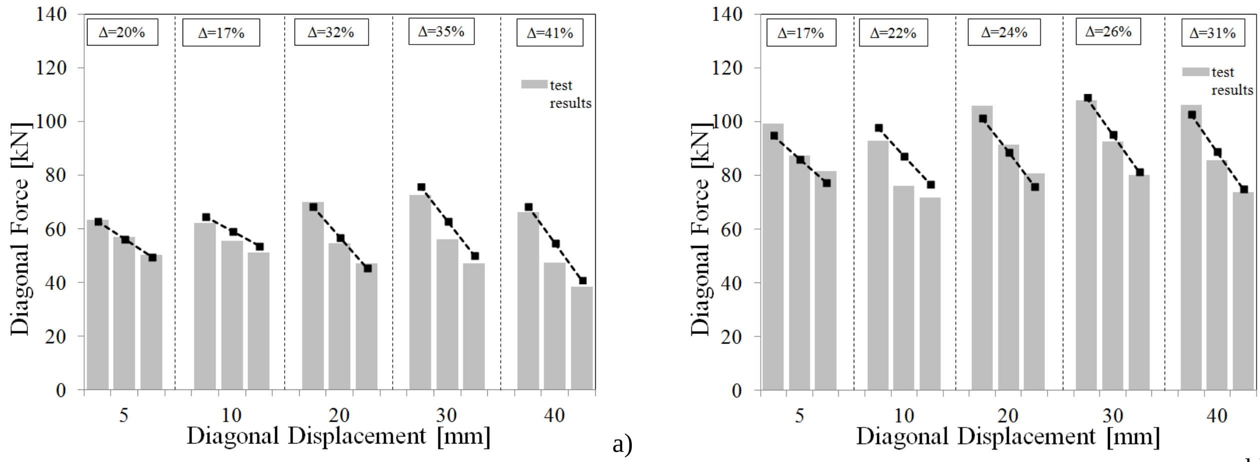

a) b)

Figure 11. Experimental vs. analytical (eq.1) strength for specimen (a) PSP1 and (b) PSP2.

The analysis of the obtained results puts into evidence some significant outcomes; firstly, it has been noticed that in order to recover the strength detriment achieved after three cycles at a certain level of strain demand, it is necessary to impose an increase of diagonal displacement of more than 5 mm.
Also, it must be observed that the panel characterized by larger perforations (PSP1) presented, apart from an expected reduced strength, a lower ductility, intended as the inelastic deformation capacity for which a strength decay is observed (6% shear strain for PSP1 versus 9% shear strain for PSP2).
Furthermore, it has been found that the strengths measured for each shear demand, when the number of cycles increases, are basically aligned on a straight line. This allowed to determine a close form analytical formulation, given in eq. (1), able to reproduce, with good approximation, the measured experimental values of diagonal forces, as is it also shown in figure 11.

$$F_{diag}=-0.0024 \cdot d^3+0.14 \cdot d^3-1.55 \cdot d+F_{y,diag}-a \cdot n \tag{1}$$

In the above equation F_{diag} is the diagonal force corresponding to the diagonal displacement d, $F_{y,diag}$ is the diagonal force corresponding to yielding, n is the number of performed cycles, a is a coefficient., which is a measure of the strength decay due to low cycle fatigue. The latter must be investigated for each panel geometry, as it relies on the slenderness of the plate portions between by perforations, according to the shear demand that is expected on the system. As for the tested specimens, PSP1 gave back values of a equal to 6.52, 5.42, 11.37, 12.81 and 13.79 for diagonal displacements of 5 mm, 10 mm, 20 mm, 30 mm and 40 mm. Instead, for specimen PSP2, a was assumed as 8.75, 10.45, 12.69, 13.87, 18.87 for diagonal displacements of 5 mm, 10 mm, 20 mm, 30 mm and 40 mm, respectively. The above equation is valid under the hypothesis, not investigated during the tests, that after three cycles, the strength decay is negligible.
Finally, in order to measure the loss of dissipative capacity due to pinching effects, the ratio F_{pinc}/F_{max} (averaged on the three cycles performed for each shear strain demands) of the diagonal force corresponding to a zero displacement (F_{pinc}) by the maximum diagonal force (F_{max}) measured on each cycle is given in Table 1. This parameter can be seen as a measure of the potential dissipative capacity

that is (ideally) maximum when a unitary value of such a value is attained. As it can be observed, for the tested shear panels the loss of dissipative capacity is significant.

Table 1. The average value of the F_{max}/ F_{pinc} ratios for several diagonal displacement demands.

Tested Specimen	Fpinc/Fmax (-) for each hysteretic cycle at displacement (mm)=				
	5	10	20	30	40
PSP 1	0.28	0.31	0.25	0.20	0.16
PSP 2	0.27	0.32	0.21	0.17	0.15

4. THE NUMERICAL MODEL

4.1 Modelling assumptions

Tested shear panels were modelled through the Abaqus [26] finite element software.

It is necessary to underline that the complexity of the buckling phenomena evidenced during the tests required a more careful approach in the modelling phase, compared with previous numerical models applied by the authors [27, 28, 29], also for those cases of perforated thin elements [30].

For the base plate in shear, the 6-node triangular thin shell (named as STRI65 in Abaqus), with five degrees of freedom per node, was used around the perforations, whereas the general purpose shell S8R, elements with 8-node and reduced integration, were adopted, close to the edges. The NLGEOM parameter has been imposed in order to allow large rotations and the stiffness matrix updating process.

The meshing algorithm was based on the assumption that, at least, two elements had to be present transversally to the plate portions between perforations, whereas a less refined mesh (average size of 25 mm) was considered at the panel edges.

A preliminary evaluation was done for the hourglass control stiffness factor ($r_{\theta}G$) to be assumed, considering not only the effect of the material shear elastic modulus (G), but also the influence of the plate thickness (t), according to eq. (2)

$$\left(r_{\theta}G\right) = 0.00375 \frac{12\int_{-t/2}^{t/2} Gt^{2}\ dt}{t^{3}} \tag{2}$$

In the case being (t=2.5 mm and G=79230 MPa) the above factor was equal to 279.

As for the members of the articulated steel frame in which the panels were included, the three-dimensional beam element B31 were adopted. All the members were connected by means of the three-dimensional two-nodes hinge connector elements CONN3D2, while the whole external frame and the plate zones included into the steel arms were restrained towards the out-of plane deformations by means of effective boundary conditions. The bottom point of the surrounding frame was fixed to the ground. The frame-to-panel connection was imposed by using the TIE constraint of the Abaqus program library, which was applied between the panel edges and the corresponding frame members. As observed by the analysis of the experimental results, this type of assumption is justified by the fact that the lateral movements between the plate and the frame members are negligible.

In figure 12, the model used for panel PSP1 is described, together with an enlarged swatch that allows to appreciate the type of meshing algorithm adopted.

4.2 Material modelling

The mechanical features of the base material were modelled accounting for its actual non linear behaviour. According to the outcomes of the performed uniaxial tensile tests described in figure 3, an average stress-strain relationship was initially considered. Then it was transformed in terms of true characteristics in order to take into account correctly the effects of finite deformations.

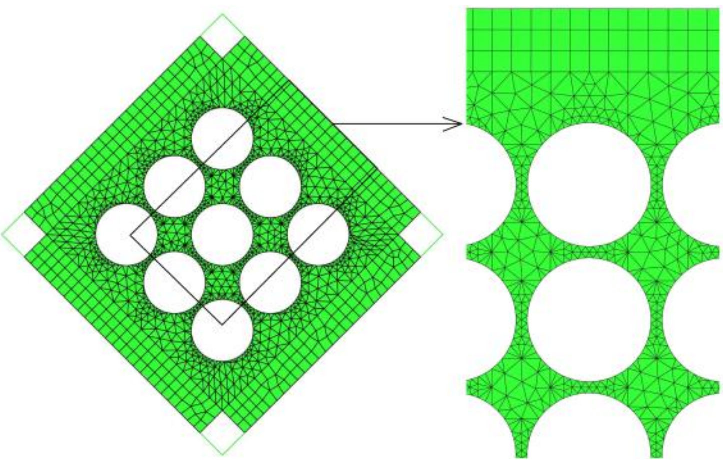

Figure 12. The adopted finite element model (PSP1 specimen)

4.3 Imperfection modelling

The experimental tests evidenced several buckling modes, affecting the panel deformation at both global and local level, which needed to be correctly stimulated by adequate initial imperfections, in order to capture the correct inelastic behaviour. In particular, it was observed that, apart from the buckling waves along the panel diagonals, the lateral torsion buckling of the plate portions between perforations significantly influenced the hysteretic response of the system.

On the other hand, a preliminary study for better understanding the importance of initial imperfections was carried out on the model shown in figure 13a. It represents a simplification of the plate portions involved in the above described instability modes. On the bottom edge, the model was fixed to the ground, whereas the top was subjected to pseudo-static analysis, according to the lateral displacements cyclic load history depicted in figure 13b, and restrained with respect to the other degrees of freedom. The analysis has been carried out firstly on the model without out-of-plane deformations and then by imposing an initial deformation given by the twisted shape corresponding to the first critical mode shown in figure 13c. In order to emphasize the influence of the above imperfection a maximum amplitude of 10 mm, which is higher than the out of plane displacements registered on the base plate of the studied panels, was considered as a limit condition. The results given in figure 13d, in terms of shear force vs. shear strain, showed that the above imperfections could provoke significant detrimental effects, with a reduction of strength and with cycles that are not stable due to the cumulated plastic deformations.

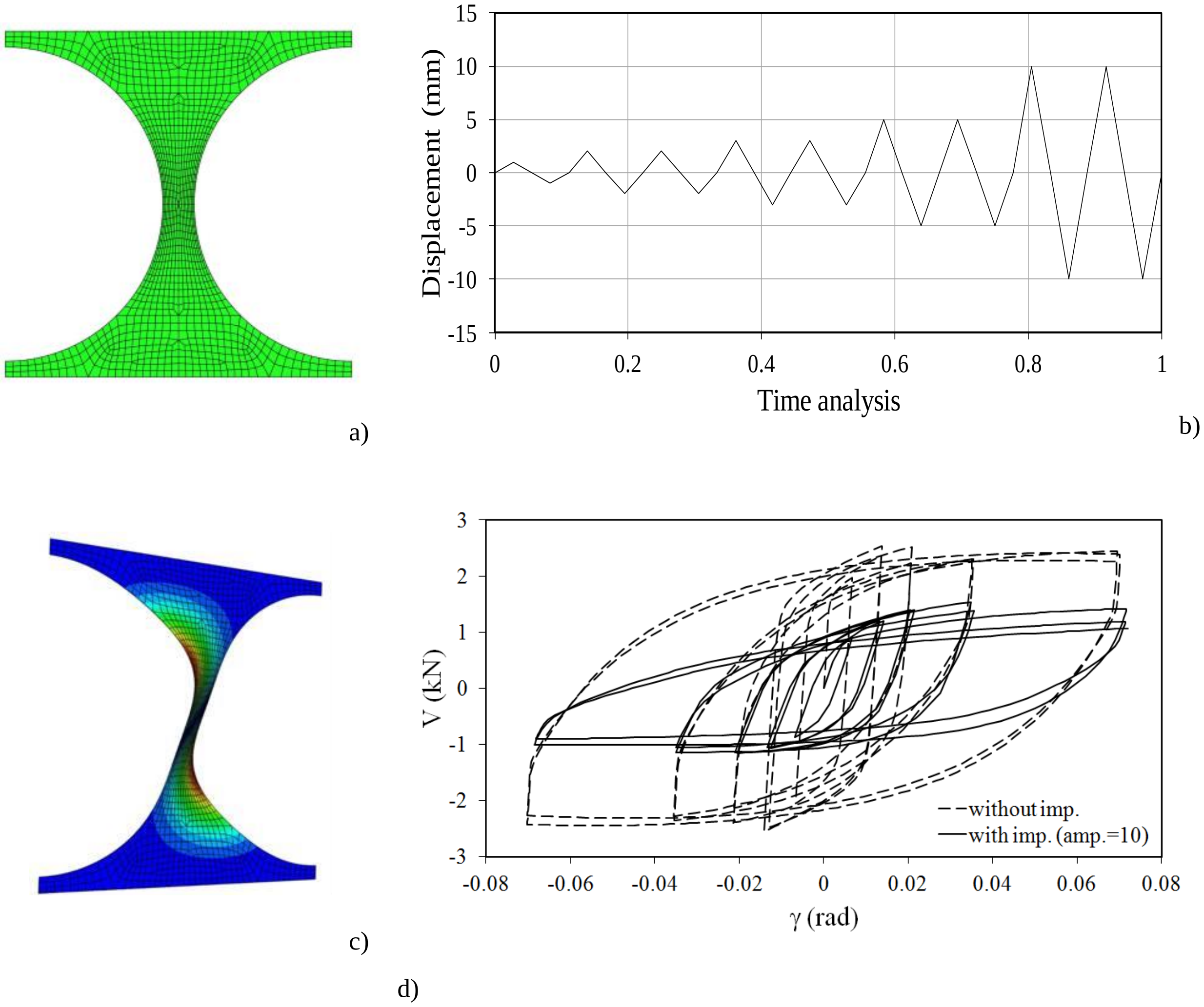

Figure 13. Imperfection sensitivity analysis on a plate portion included between perforations: a) model meshing; b)imposed lateral displacement history; c) imposed initial imperfections (maximum amplitude of 10 mm); d) obtained results

For this reason, the critical mode shapes shown in figure 14 were superimposed in order to get the initial deformation of the plates. These lead to have both out-of–plane deformations along the two diagonals of the panel and simultaneously a twisted shape for the plate portions included between two perforations.

An amplitude of 2.5 mm, namely the plate thickness, was imposed for the maximum out-of-plane displacement of the plate, as it was judged reasonable.

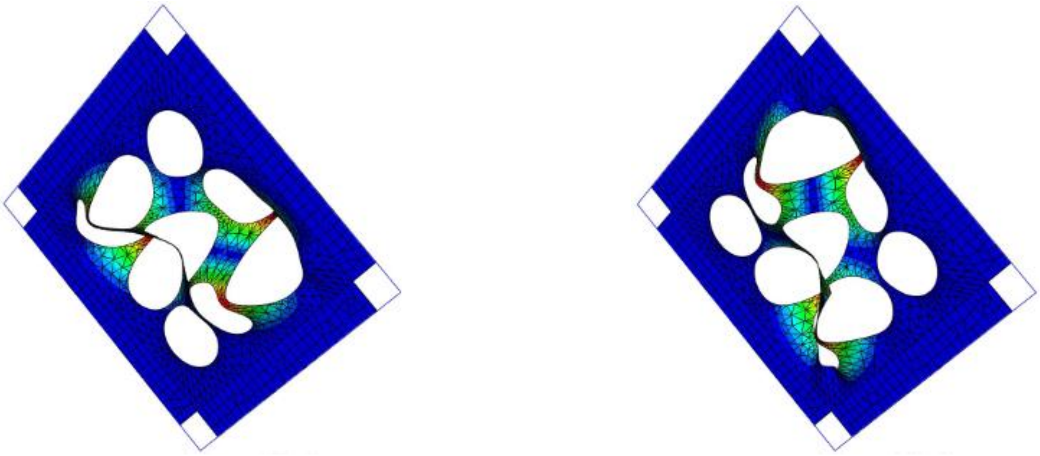

Figure 14. The two deformed shapes superimposed for modelling the initial imperfection of the plate

It must be underlined that the reliability of the proposed models was also corroborated by sensitivity analyses conducted with respect to all the other modelling assumptions described previously (i.e. finite element typology, mesh size, etc), that allowed to consider the obtained results stable.

4.4 Numerical vs. experimental results

A standard pseudo-static cyclic analysis was carried out for reproducing the experimental tests. To this purpose, the same diagonal displacements history used during the experimental analysis, depicted in figure 4, was imposed to the top node of the model.

The comparison between the obtained results, shown in figure 15 in terms of diagonal displacement vs. diagonal force, proved that the adopted approach is reliable enough for using the considered FEM model with the aim of carrying out parametric analyses. In fact all the main behavioural features of the tested plates, namely strength, stiffness, ductility, dissipative capacity and strength decay, were perfectly reproduced for each shear demand.

Furthermore, the analysis of the internal stresses at several shear demands allowed to better interpret some of the observed experimental evidences.

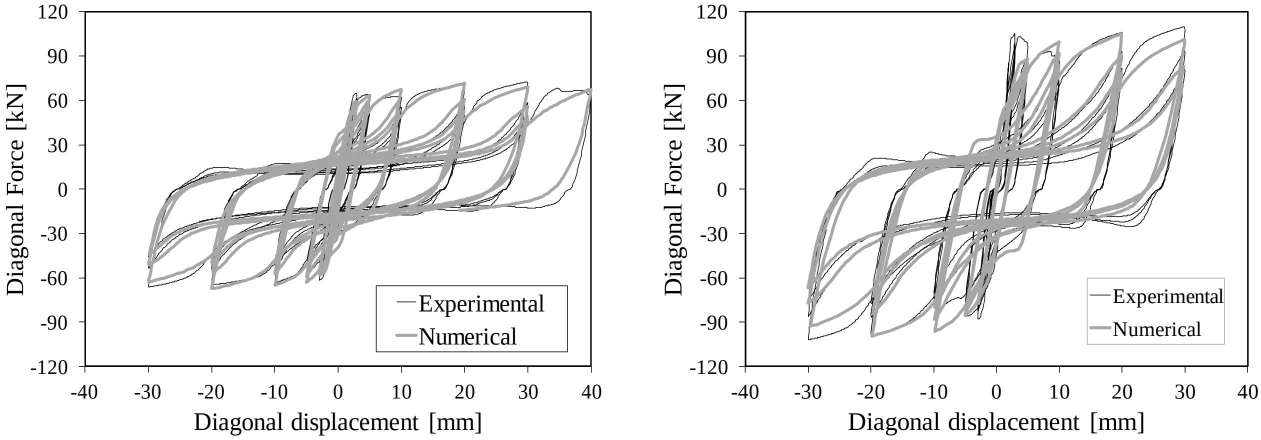

a)

b)

Figure 15. Numerical vs. Experimental results for shear panels PSP-1 (a) and PSP-2 (b)

For example, the stress pattern shown for specimen PSP2 in figure 16, corresponding to a diagonal displacement demand of 10 mm, allowed to understand that the rotation of the principal stress at the bottleneck of the panel portions included within two consecutive perforations originated bending moment that lead to the lateral-torsion buckling phenomena discussed in Section 3.2.

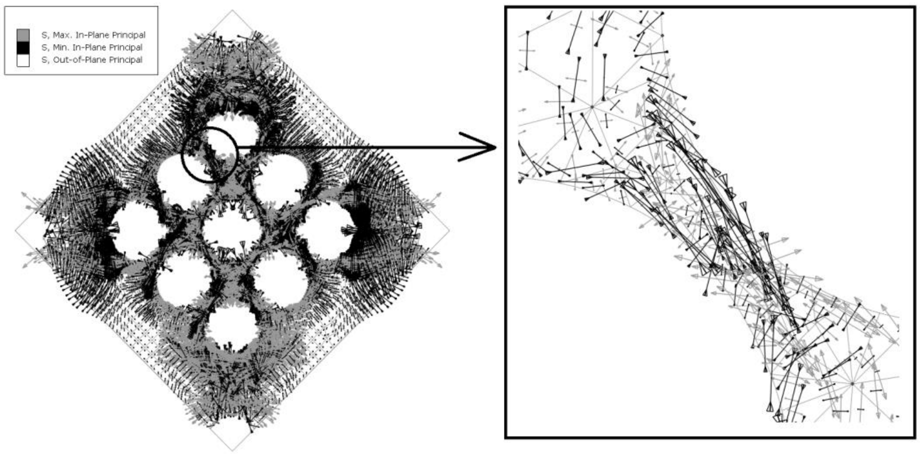

Figure 16. Internal principal stresses for specimen PSP-2 (diagonal displacement demand of 10 mm - shear strain of 2.2%)

5. PARAMETRIC ANALYSIS

5.1 General

A parametric analysis has been carried out varying the number of perforations, with the main purpose to provide an analytical tool able to predict, with an acceptable approximation, the panel response depending on the main geometrical parameters influencing for the system performance. The following parameters have been considered: perforation diameter (*D*), minimum spacing between holes (*s*) and depth *e* of the not perforated area, namely the distance between the outer holes and the plate area bolted to the perimeter frame (named as constrained area). While the dissipative performance of the panel is to be ascribed to the perforated central core shown in figure 17a, the not perforated area serves to avoid negative overlapping of stresses that could lead to brittle failure mechanism. On the other hand, it allows a strength resource for the overall resistance of the perforated pate.

The three parameters *e, s* and *D* are related each others through the following expression (eq. 3):

$$e = \frac{1}{2}\left[L_p - (n_h \cdot D) - s \cdot (n_h - 1)\right] \tag{3}$$

where L_p is the width of the free area of the panel and n_h is the number of perforations.

Moreover *e* and L_p give the parameter ξ, reported in eq. (4), that is strongly related to the influence of perforations on the dissipative capacity of the shear panel.

$$\xi = 1 - \frac{2 \cdot e}{L_p} \tag{4}$$

When ξ is 0, the panel performance coincides with the one of a solid plate, while ξ=1 means that the *not perforated area* does not exist.

Another influencing parameter for the plate performance is the ratio between its shear net area $A_{p,net}$ and the transversal area of the corresponding A_p solid plate (see eq. 5), which is strictly related to the actual shear strength of the plate.

$$\frac{A_{p,net}}{A_p} = \frac{L_p - n_h \cdot D}{L_p} \tag{5}$$

The parametric analysis has been carried out considering twenty-two geometries described in table 2, which have been obtained by varying the above parameters.

Among the studied cases also the solid panel (ξ=0) has been considered, as for this specimens an experimental test was preliminarily carried out [31]. The comparison between the cyclic response retrieved during this test and the numerical results (see figure 17.b), proves the reliability of the proposed model in capturing the real system response also in absence of perforations.

Table 2: Geometrical features of the perforated shear panels considered for the parametric analysis.

Specimen	n_h (-)	D (mm)	s (mm)	e (mm)	$A_{p,net}/A_p$ (%)	D/s (-)	ξ (-)
Not-perforated	0	0.00	0.00	255.00	100.0	0.00	0.00
PSP 1	3	127.50	12.75	51.00	25.0	10.00	0.80
PSP 2	3	107.40	42.90	51.00	36.8	2.50	0.80
M 2x2-D87	2	87.00	50.00	143.00	65.9	1.74	0.44
M 3x3-D32	3	31.88	63.79	143.40	81.3	0.50	0.44
M 3x3-D51	3	51.27	51.00	127.50	69.8	1.01	0.50
M 3x3-D100	3	100.00	10.00	95.00	41.2	10.00	0.63
M 3x3-D109	3	109.29	12.14	78.93	35.7	9.00	0.69
M 3x3-D128	3	127.63	10.00	53.55	24.9	12.76	0.79
M 3x3-D131	3	130.98	5.00	53.55	23.0	26.20	0.79
M 4x4-D72	4	71.94	21.48	78.90	43.6	3.35	0.69
M 4x4-D99	4	98.84	2.28	53.90	22.5	43.35	0.79
M 5x5-D48	5	48.29	27.54	79.20	52.7	1.75	0.69
M 5x5-D74	5	74.00	8.26	53.48	27.5	8.96	0.79
M 5x5-D81	5	81.00	3.00	46.50	20.6	27.00	0.82
M 5x5-D85	5	85.00	15.00	12.50	16.7	5.67	0.95
M 5x5-D90	5	90.00	10.00	10.00	11.8	9.00	0.96
M 5x5-D95	5	95.00	5.00	7.50	6.9	19.00	0.97
M 9x9-D27	9	26.62	20.34	53.90	53.0	1.31	0.79
M 9x9-D43	9	42.50	7.50	33.75	25.0	5.67	0.87
M 9x9-D45	9	45.00	5.00	32.50	20.6	9.00	0.87
M 9x9-D48	9	47.50	2.50	31.25	16.2	19.00	0.88

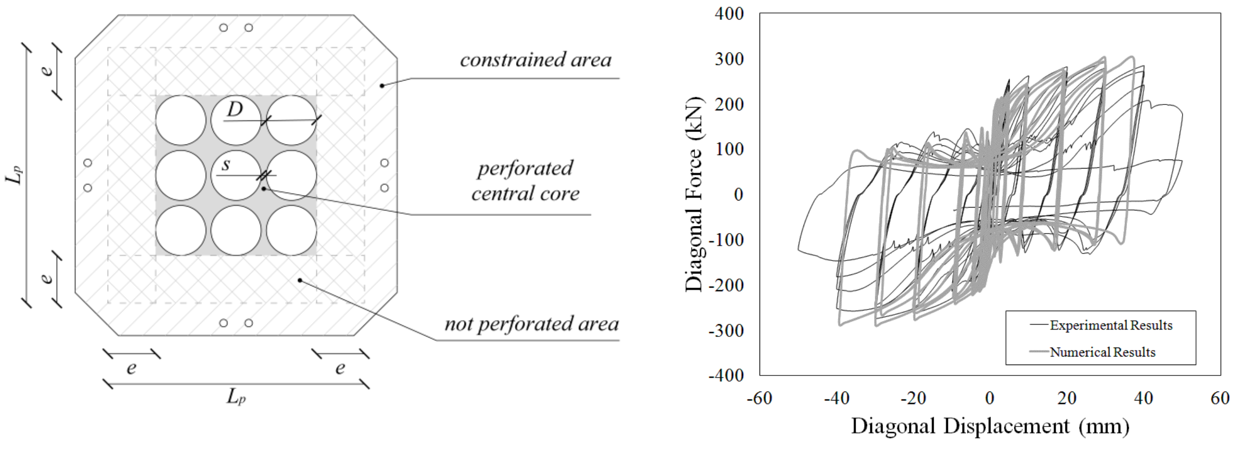

a)

b)

Figure 17. a) Geometrical parameters influencing the perforated panel response. b) comparison between the experimental and numerical results for solid panel (ξ=0) [31]

5.2 Proposed design rules

In figure 18 the obtained maximum shear strength, F_{max} conventionally normalised to the yielding shear strength computed for the solid panel according to Thorburn et al. [32], is given as a function of the ratio A_{pnet}/A_p.

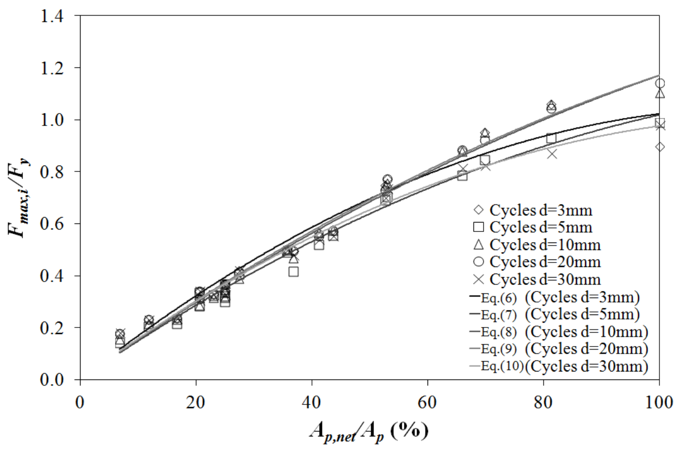

Figure 18. The parametric analysis results in terms F_{max}/ F_y compared with the analytical values given by eqs (6-10)

As it is possible to observe, the obtained results are well fitted, for each shear strain, by curves for which simple analytical expressions could be given. These are reported in the following eqs. (6), (7), (8), (9) and (10) for shear strains of 0.66% (diagonal displacements d=3 mm), 1.1% (d=5 mm), 2.2% (d=10 mm), 4.4% (d=20 mm) and 6.6 (d=30 mm), respectively.

$$\frac{F_{\max,0.7\%}}{F_y} = -7 \cdot 10^{-5} \cdot \left(\frac{A_{p,net}}{A_p}\right)^2 \cdot 0.0176 \cdot \frac{A_{p,net}}{A_p} \tag{6}$$

$$\frac{F_{\max,1.1\%}}{F_y} = -5 \cdot 10^{-5} \cdot \left(\frac{A_{p,net}}{A_p}\right)^2 \cdot 0.0153 \cdot \frac{A_{p,net}}{A_p} \tag{7}$$

$$\frac{F_{\max,2.2\%}}{F_y} = -4 \cdot 10^{-5} \cdot \left(\frac{A_{p,net}}{A_p}\right)^2 \cdot 0.0157 \cdot \frac{A_{p,net}}{A_p} \tag{8}$$

$$\frac{F_{\max,4.4\%}}{F_y} = -4 \cdot 10^{-5} \cdot \left(\frac{A_{p,net}}{A_p}\right)^2 \cdot 0.0160 \cdot \frac{A_{p,net}}{A_p} \tag{9}$$

$$\frac{F_{\max,6.6\%}}{F_y} = -4 \cdot 10^{-5} \cdot \left(\frac{A_{p,net}}{A_p}\right)^2 \cdot 0.0153 \cdot \frac{A_{p,net}}{A_p} \tag{10}$$

At the same manner, it has been observed that linear equations (11), (12), (13) and (14) allow to predict, respectively for shear strains of 1.1% (d=5 mm), (d=10 mm), (d=20 mm) and (d=30 mm), the ratio F_{pinc}/F_{max}, as a function of both the ratio D/s and the parameter ξ, as it is shown in figure 19.

$$\frac{F_{pinc,1.1\%}}{F_{\max,5}} = 0.001 \cdot \left(\frac{D}{s}\right) + 0.02 \cdot \xi + 0.45 \tag{11}$$

$$\frac{F_{pinc,2.2\%}}{F_{\max,10}} = -0.004 \cdot \left(\frac{D}{s}\right) + 0.04 \cdot \xi + 0.32 \tag{12}$$

$$\frac{F_{pinc,4.4\%}}{F_{\max,20}} = 0.008 \cdot \left(\frac{D}{s}\right) + 0.05 \cdot \xi + 0.21 \tag{13}$$

$$\frac{F_{pinc,6.6\%}}{F_{\max,30}} = 0.008 \cdot \left(\frac{D}{s}\right) + 0.05 \cdot \xi + 0.186 \tag{14}$$

All the above equations can be profitably used for selecting the most performing perforated shear panel when a certain deformation is expected under a design earthquake. The possibility of predicting magnitudes that are strongly related to the dissipative capacity of the system makes the above formulations particularly useful when a displacement based design approach is adopted. In fact, once that the target storey drift is established for each storey of the frame in which panels are installed, the related shear strain of the panel is approximately given by a scale factor equal to the ratio between the height of the storey and the height of the panel itself.

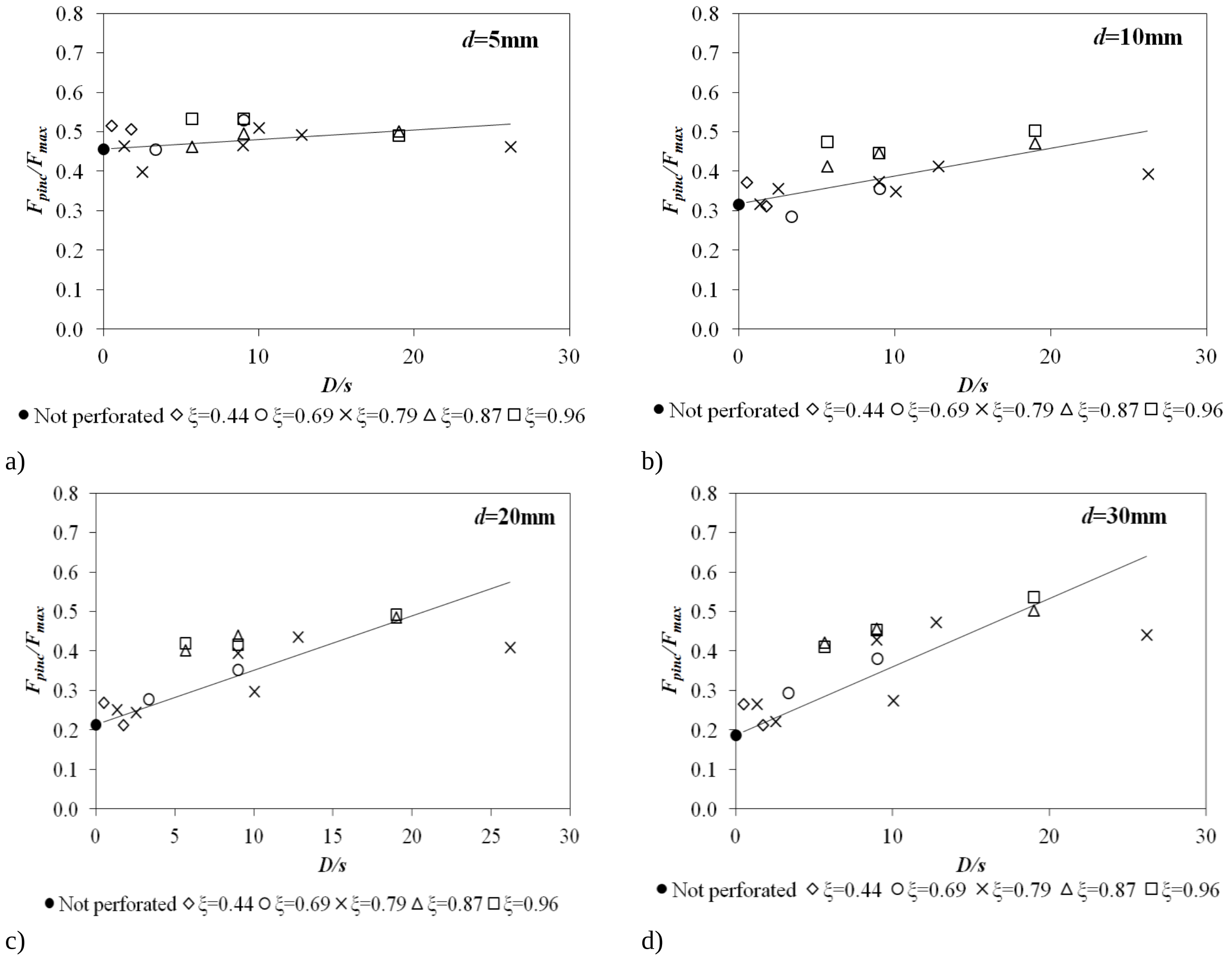

Figure 19. a) The parametric analysis results in terms F_{max}/ F_{pinc} compared with the analytical values given by eqs (9-12)

6. CONCLUSIONS

This paper presented an experimental and numerical study carried out on perforated shear panels to be used for the seismic protection of framed buildings. The main conclusions, based on both the experimental evidences and the outcomes obtained by the use of a calibrated FEM model, are synthetically listed in the following:

- The perforations applied on the base plate, when properly conceived, induce a variation of the internal stress pattern, which allows to mitigate the effects of those critical modes that could develop along the diagonals (usually limiting the performance of solid thin plates);

- The dissipative performance of perforated plates could be negatively influenced by the presence of local lateral –torsion buckling when the plate portions included within two perforations are too much slender, due to a rotation of the principal stresses that produce bending moment;
- For large shear demands, the above local buckling phenomena could produce cumulated inelastic stresses that provoke detrimental effects on the strength when the number of cycles increases;
- It is possible to predict the strength of the panels for each shear demand once the influence of the aforementioned cumulated inelastic stresses is known, which depends on the plate geometry;
- The use of the proposed design formulations allows to optimize the geometrical features of the system, in order to maximize both maximum inelastic strength and dissipative capacity.

Acknowledgements

This study was developed in the framing of the ReLUIS Italian research project. The authors wish to thank Eng. Giuseppe Campanella and Eng. Emanuele Scaiella for their precious support in laboratory tests.

REFERENCES

[1] De Matteis, G., Formisano, A., Mazzolani, F.M. An innovative methodology for seismic retrofitting of existing RC buildings by metal shear panels (2009) Earthquake Engineering and Structural Dynamics, 38 (1), pp. 61-78.

[2] Formisano, A., De Matteis, G., Mazzolani, F.M. Numerical and experimental behaviour of a full-scale RC structure upgraded with steel and aluminium shear panels (2010) Computers and Structures, 88 (23-24), pp. 1348-1360.

[3] De Matteis, G., Formisano, A., Mazzolani, F.M., Panico, S. Design of low-yield metal shear panels for energy dissipation (2005) Improvement of Buildings' Structural Quality by New Technologies - Proceedings of the Final Conference of COST Action C12, pp. 665-675.

[4] Nakashima, M. “Strain-hardening behavior of shear panels made of low-yield steel. I: test” (1995) Journal of structural engineering New York, N.Y., 121 (12), pp. 1742-1749.

[5] De Matteis, G., Mazzolani, F.M., Panico, S. “Experimental tests on pure aluminium shear panels with welded stiffeners” (2008) Engineering Structures, 30 (6), pp. 1734-1744.

[6] De Matteis G., Brando G., Panico S., Mazzolani F.M., “Bracing type pure aluminium stiffened shear panels: An experimental study” (2009) Advanced Steel Construction, 5 (2), pp. 106-119.

[7] De Matteis, G., Brando, G., Mazzolani, F.M. “Pure aluminium: An innovative material for structural applications in seismic engineering” (2012) Construction and Building Materials, 26 (1), pp. 677-686

[8] Rai, D.C. Inelastic cyclic buckling of aluminium shear panels (2002) Journal of Engineering Mechanics, 128 (11), pp. 1233-1237.

[9] Jain, S., Rai, D.C., Sahoo, D.R. “Postyield cyclic buckling criteria for aluminum shear panels” (2008) Journal of Applied Mechanics, Transactions ASME, 75 (2), pp. 0210151-0210158.

[10] Brando, G., D'Agostino, F., De Matteis, G. “Experimental tests of a new hysteretic damper made of buckling inhibited shear panels” (2013) Materials and Structures/Materiaux et Constructions, 46 (12), pp. 2121-2133.

[11] De Matteis, G., D’Agostino, F., Brando, G. “Experimental tests on steel buckling inhibited shear panels” (2014) Open Construction and Building Technology Journal, 8, pp. 279-288.

[12] Deng, K., Pan, P., Li, W., Xue, Y. “Development of a buckling restrained shear panel damper” (2015) Journal of Constructional Steel Research, 106, pp. 311-321.

[13] Brando G., D'Agostino F., and De Matteis G. “Seismic performance of MR frames protected by viscous or hysteretic dampers”, (2014). Struct. Design Tall Spec. Build., doi: 10.1002/tal.1204.

[14] Hitaka, T., Matsui, C. “Experimental study on steel shear wall with slits” (2003) Journal of Structural Engineering, 129 (5), pp. 586-595.

[15] Pohlenz, A. J., (2010) “Development of Steel Slit Wall Dampers with Embedded Condition Assessment Capabilities”, Ph.D. thesis, University of Kyoto, Japan.

[16] Vian, D., Bruneau, M., Purba, R.. “Special perforated steel plate shear walls with reduced beam section anchor beams. II: Analysis and design recommendations” (2009) Journal of Structural Engineering, 135 (3), pp. 221-228.

[17] Valizadeh, H., Sheidaii, M., and Showkati, H. “Experimental investigation on cyclic behaviour of perforated steel plate shear walls.” (2012) Journal of Constructional Steel Research. 70 308-316.

[18] Alavi, E., Nateghi, F. “Experimental study on diagonally stiffened steel plate shear walls with central perforation”(2013) Journal of Constructional Steel Research, n.89, pp. 9–20.

[19] Chan, R.W.K., Albermani, F., Kitipoirnchai, S. “Experimental study of perforated yielding shear panel device for passive energy dissipation” (2013) Journal of Constructional Steel Research, n.91, pp. 14–25.

[20] Purba, R., Bruneau, M. Finite-element investigation and design recommendations for perforated steel plate shear walls (2009) Journal of Structural Engineering, 135 (11), pp. 1367-1376.

[21] Bhowmick, A.K. Seismic behavior of steel plate shear walls with centrally placed circular perforations (2014) Thin-Walled Structures, 75, pp. 30-42.

[22] Pellegrino, C., Maiorana, E., Modena, C. Linear and non-linear behaviour of steel plates with circular and rectangular holes under shear loading (2009) Thin-Walled Structures, 47 (6-7), pp. 607-616.

[23] Maurya, A., Egorova, N., Eatherton, M.R. Development of ring-shaped steel plate shear walls (2013) Structures Congress 2013: Bridging Your Passion with Your Profession - Proceedings of the 2013 Structures Congress, pp. 2971-2982.

[24] Egorova, N., Eatherton, M.R., Maurya, A. Experimental study of ring-shaped steel plate shear walls (2014) Journal of Constructional Steel Research, 103, pp. 179-189.

[25] ECCS-CECM. Recommended testing procedure for assessing the behaviour of structural steel elements under cyclic loads, 1985.

[26] Dassault Systemes Simulia Corporation. Abaqus, User’s manual-version 6.7 documentation; 2007.

[27] Brando, G., De Matteis, G. Experimental and numerical analysis of a multi-stiffened pure aluminium shear panel (2011) Thin-Walled Structures, 49 (10), pp. 1277-1287.

[28] Brando, G., De Matteis, G. Design of low strength-high hardening metal multi-stiffened shear plates (2014) Engineering Structures, 60, pp. 2-10.

[29] De Matteis, G., Landolfo, R. Modelling of lightweight sandwich shear diaphragms for dynamic analyses (2000) Journal of Constructional Steel Research, 53 (1), pp. 33-61

[30] Brando, G., De Matteis, G. Buckling resistance of perforated steel angle members (2013) Journal of Constructional Steel Research, 81, pp. 52-61.

[31] Sarracco, G. “Numerica and Experimental Behaviour of Perforated Steel Plate Shear Panels” (2015), Ph.D thesis. Department of Engineering and Geology, University “G.d’Annunzio” of Chieti-Pescara, Italy. April, 2015.

[32] Thorburn, J. L., Kulak, G. L:, Montgomery, C. J. “Analysis of Steel Plate Shear Walls” (1983), Structural Engineering Report No. 107, Department of Civil Engineering, University of Alberta, Edmonton, Alberta.